Atmospheric pressure air plasma treatment to improve the 3D printing of polyoxymethylene

Ignacio Muro-Fraguas[1], Elisa Sainz-García[1], Alpha Pernía-Espinoza[1], Fernando Alba-Elías[1*]

[1] Department of Mechanical Engineering. University of La Rioja. c/ Luis de Ulloa 20, 26004 Logroño, La Rioja, Spain.

Accepted Version for publication in Plasma, Processes and Polymers

Link to publisher version (DOI): https://doi.org/10.1002/ppap.201900020

Published source citation:

Muro-Fraguas, I., Sainz-García, E., Pernía-Espinoza, A., & Alba-Elías, F. (2019). Atmospheric pressure air plasma treatment to improve the 3D printing of polyoxymethylene. Plasma Processes and Polymers, 16(7). https://doi.org/10.1002/PPAP.201900020

Article type: Full Paper

Atmospheric pressure air plasma treatment to improve the 3D printing of polyoxymethylene

Ignacio Muro-Fraguas, Elisa Sainz-García, Alpha Pernía-Espinoza, Fernando Alba-Elías*

_____

Ignacio Muro-Fraguas

Department of Mechanical Engineering

University of La Rioja

C/ Luis de Ulloa 20, 26004 - Logroño, La Rioja, Spain.

Tel.: +34 941299276; fax: +34 941299794.

E-mail address: ignacio.muro@unirioja.es

Dr. Elisa Sainz-García

Department of Mechanical Engineering

University of La Rioja

C/ Luis de Ulloa 20, 26004 - Logroño, La Rioja, Spain.

Tel.: +34 941299276; fax: +34 941299794.

E-mail address: elisa.sainzg@unirioja.es

Dr. Alpha Pernía-Espinoza

Department of Mechanical Engineering

University of La Rioja

C/ Luis de Ulloa 20, 26004 - Logroño, La Rioja, Spain.

Tel.: +34 941299276; fax: +34 941299794.

E-mail address: alpha.pernia@unirioja.es

Dr. Fernando Alba-Elías

Department of Mechanical Engineering

University of La Rioja

C/ Luis de Ulloa, 20, 26004 - Logroño, La Rioja, Spain.

Tel.: +34 941299276; fax: +34 941299794.

E-mail address: fernando.alba@unirioja.es

All the authors contributed equally to this work.

_____

Polyoxymethylene (POM), an excellent engineering material, shows drawbacks as a 3D printing material:[a] difficulties in the adhesion of the first printed layer and [b] thermal contractions during printing. In this work, an atmospheric pressure air plasma treatment is applied on a polycarbonate (PC) printing base. The effect of the plasma treatment parameters is studied. Chemical and morphological tests are conducted. Results shows that, in general, as the plasma exposure rises, so does the degree of oxidation of the PC surface and the adhesion of POM. However, care must be taken as thermal residual stresses may reduce adhesion. Finally, an increase in adhesion of up to 45% is achieved.

1 Introduction

The high-speed development of additive manufacturing (AM) today is creating a completely new path in the fabrication of components. Parts that have complex geometries and cavities, and are impossible to manufacture by traditional methods, may be produced adding layer-upon-layer by AM.[1,2] Although there are more than ten different types of materials for AM,

the most popular ones are polylactic acid (PLA), of vegetal origin, and acrylonitrile butadiene styrene (ABS), a petroleum derivate.[3] Nevertheless, the search for new materials continues. Polyoxymethylene (POM), also known as acetal, polyacetal and polyformaldehyde, is considered to be an engineering material that is competitive with a number of plastics (such as nylon) and metals, because of its light weight, low friction, low hygroscopicity, excellent wear resistance, outstanding dimensional stability, high tensile strength, impact resistance, stiffness, fatigue endurance and wide end-use temperature range.[4] In addition to its excellent mechanical and thermal properties, it is also chemical resistant to most solvents, chemicals and fuels at room temperature.[5] Although POM is similar to nylon in many respects, it is considered to be superior in creep resistance, fatigue endurance, stiffness and hygroscopy. Some physical, mechanical and thermal properties of POM are compared to those of nylon 6 and ABS in Table 1.[4,6–10]

Property	**POM**	**Nylon 6**	**ABS**
Density	1400 kg/m^3	1140 kg/m^3	1040 kg /m^3
Elasticity module	2.8 GPa	2.3 GPa	2.1 GPa
Creep tension	65 MPa	50 MPa	35 MPa
Flex module	2.7 GPa	2.2 GPa	2.1 GPa
Maximum elongation	30%	71%	34%
IZOD Impact (23ºC)	54 J/m	106 J/m	128 J/m
Friction coefficient against steel	0.1 (static) 0.2 (dynamic)	0.2 (static) 0.4 (dynamic)	0.3 (static) 0.5 (dynamic)
Melting temperature	182 ºC	230 ºC	220 ºC
Flex temperature under load	110 ºC	160 ºC	88 ºC
Decomposition temperature	>290 ºC	>280 ºC	>260 ºC
Shrinkage ratio in molding	2.2%	1.2%	0.7%

Table 1. Properties of POM, Nylon 6 and ABS.

POM has been processed traditionally by injection molding, extrusion and subtractive manufacturing (machining). Nevertheless, among the AM processes, fused deposition modeling (FDM) offers an appropriate technology for the manufacture of POM parts.[1] POM can be easily extruded at temperatures below 250ºC, which can be achieved with most 3D

printers. Also, the use of a heated printing base and an enclosure, which can be easily implemented in any 3D printer, will provide favorable conditions for crystallization. In addition, FDM is a clean and easy-to-use technology.

Nonetheless, despite the aforementioned advantages, world-renowned 3D printing companies, such as *Stratasys* and *3D systems,* provide neither parts-on-demand using POM nor supply POM as 3D printing filament.[9,11] Apart from these industry-oriented-companies, the top globally recognized 3D printing filament suppliers that are oriented to 3D desktop printing are also providers of engineering material filaments for industrial applications, such as ColorFabb, Hatchbox, Filamentum, Taulman3D, 3DFilaPrint and Formfutura, but do not promote either POM filament within their products.[12–17] Even DuPont, the company that first synthesized a version of POM and that has recently bet on the emerging 3D printing filament market, does not include POM filament within its offer.[6] In view of this evidence, it is not too risky to claim that POM is not an easy material to print with consistent and reliable results. Only a few companies provide POM as a 3D printing filament with guarantees. They include Gizmo Dorks, Actifil3D, Apium and FFF World.[18–21]

Two main issues to take care of are generally mentioned by these suppliers. First, the self-lubricating nature of POM makes the adhesion of the first printed layer on the printing base quite difficult to achieve.[22] To that end, it is advisable to print using a heated-base with a temperature that exceeds 130ºC. Thus, the deposited filament will have a temperature that is near the melting point, which favors the adhesion. Nevertheless, this is a rather high temperature that most of the desktop 3D printers cannot reach (the common maximum heated-base temperature is 100ºC). In any case, the use of a strong adhesive (print glue, ABS slurry, etc.) seems to be an indispensable requirement for ensuring the first layer adhesion. Secondly, the printed part could experience severe dimensional changes due to thermal contraction during uneven cooling (an effect commonly known as warping). The caused could be that POM has more than three times the shrinkage ratio of ABS (see **Table 1**), which also is

affected by warping. Thus, the use of a preheated enclosure and a heated base is strongly recommended to overcome warping.

Considering the above-mentioned difficulties in printing POM material, this article proposes the use of the cold atmospheric plasma treatment in order to improve adhesion of the part's first layer and, consequently, the quality of the POM printed part. In addition, Polycarbonate (PC) is one of the most useful plastic substrate materials due to its reduced weight, transparency and high shock resistance.[23,24] Atmospheric cold plasma has proven to be a versatile surface treatment for PC as it can modify the polymer surface without affecting its bulk properties.[25,26]

Many studies have shown the adhesion improvement after a plasma treatment in different fields, which is due mainly to modification of the solid surface (cleaning, etching or surface activation).[27–32] This means that plasma technology has been used widely in different industrial fields. However, to the best of our knowledge, there are no studies relating to plasma treatments and the promotion of adhesion in 3D printing.

In this particular case, there are two peculiarities that give novelty to this work. On the one hand, it is remarkable that the adhesion that is intended to be promoted should not be permanent in time. Once the part is printed, it must be easily detached from the printing base. This fact makes it necessary to use special adhesives whose effectiveness is only effective at high temperatures (near to filament melting temperature) and not at room temperature in order to be able to detach de 3D printed part from the printing base. On the other hand, the filament that is intended to adhere to the printing base melts and solidifies while it comes into contact with the adhesive applied on the printing base. That is, the objective is to improve the adhesion between a solid material at 100 ºC (the PC printing base) and the POM filament, which is applied at 250 ºC in the liquid-solid state. This fact makes the plasma treatments that one could think to be more efficient (those that generate many adhesive chemical bonds) are

not effective in our particular application, since they release surface tensions, which result in a bad adhesion.

In this work, we have analyzed the effect of several parameters of the plasma treatment, such as the number of passes, the plasma jet speed, the gas flow and the plasma power, on POM adhesion to a polycarbonate (PC) substrate used as the printing base. To observe surface modifications of the PC substrate, several chemical and morphological tests were conducted. Finally, we used a pull-off test to assess the adhesion quality of the samples.

2 Experimental

2.1 Materials

The 3D printing of POM was undertaken on a thin PC sheet of 100x50x3 mm. This PC sheet was fastened to a stainless steel plate by six M4 screws in order to avoid deformation or movement of the PC base during the different phases of the process (plasma treatment, 3D printing and pull-off test) (see **Figure 1**).

Just before plasma treatment, the PC sheet was cleaned with isopropanol to eliminate any surface contamination. After plasma treatment, two layers of a roll-on adhesive (DIMAFIX) were applied manually.[33] The chemical composition of DIMAFIX is: Ethylalcohol (70-80%), Isopropylalcohol (10-15%), 1-vinyl-2-pyrrolidone-vinyl acetate polymer (10-15%) and n-butyl acetate (1-2.5%).

The 3D printing filament chosen was POM-Tech. It was provided by FFF World and made from non-recycled materials.[20]

Figure 1. Sequence of the complete process: [a] PC sheet assembling, [b] Plasma treatment, [c] DIMAFIX application, [d] PC-sheet assembling on printer base, [e] Dollies printing (two for each sheet), [f] Dollies printed and [g] Pull-off test and [h] Dolly tested.

2.2 Atmospheric Pressure Air Plasma Treatment

After the printing base was assembled (PC base and stainless steel plate –see **Figure 1a**–) and cleaned with isopropanol, it was pre-treated by Atmospheric Pressure Plasma Jet (APPJ) technology (see **Figure 1b**).

A picture and a schematic diagram of the APPJ system that was used to treat the samples is shown in **Figure 2a** and **3**, respectively. This system was developed by VITO (Flemish Institute for Technological Research). It consists of an Al_2O_3 dielectric tube between two cylindrical electrodes. The outer electrode is connected to high voltage during operation and the inner electrode is grounded.

Figure 2. [a] Plasma equipment at the University of La Rioja, [b] Ultimaker 2+ 3D printer and [c] TRIAX-50 (Controls) machine.

As **Table 2** shows, thirteen different plasma treatments were applied. Three different flows of compressed air (40, 60 and 80 slm) were used as supply gas to generate plasma. In addition, three different levels of plasma power (300, 400 and 500 W) were used at a frequency of 75 kHz to evaluate their effect. In all treatments, both the gap between the plasma discharge and the printing base (3 mm) and the track pitch of the plasma treatment (2 mm) were constant. Depending on the sample, the jet was moved across the entire printing base as many times as **Table 2** indicates (passes) at different speeds (between 20 and 50 mm/s). Each treatment was conducted four times and the average values of the results are presented herein.

Figure 3. [a] Plasma jet and [b] its schematic diagram.

Sample identification	Parameters			
	Passes	Plasma Power (W)	Plasma Jet Speed (mm/s)	Plasma Gas Flow (slm)
PC (untreated)	-	-	-	-
S20	1	500	20	60

S25	1	500	25	60
S30	1	500	30	60
S35	1	500	35	60
S40	1	500	40	60
S45	1	500	45	60
S50	1	500	50	60
P2	2	500	30	60
P3	3	500	30	60
W300	1	300	30	60
W400	1	400	30	60
F40	1	500	30	40
F80	1	500	30	80

Table 2. Sample identification according to the parameters of the plasma treatments.

2.3 3D Printing

After plasma treatment and before 3D printing, two layers of a roll-on adhesive (DIMAFIX) were applied manually (**Figure 1c**). The 3D printing machine that was used in this study was the Ultimaker 2+, which is manufactured by Ultimaker (see **Figure 2b**).[34] It is a high quality, accurate, reliable and affordable desktop 3D printer.

As it has been mentioned in the introductory section, important issues can arise when using POM as a printing material. This is why a variety of factors were considered to minimize such problems. In order to avoid warping, the use of a preheated enclosure and a heated base at a temperature that exceeds 130 ºC was recommended. However, the 3D printer used in this work was an open-structure desktop 3D printer that was unable to reach such a high temperature in its printing base. Therefore, a printing base temperature of 100ºC (the maximum stable temperature that the printer could achieve) was established for all of the studied samples. The extruder temperature was 250 ºC. In addition, a methacrylate enclosure was built in order to provide a preheated enclosure. Along with these warping prevention measures, an extension of 4 mm around the first layer edges (commonly known as brim) was printed for all samples.

Finally, in order to test the proposed treatment, a gear like geometry was adopted to be printed (see **Figure 1f**). We consider this type of geometry to be challenging for 3D-printed, since the

sharp ending sections create thermal stress concentration points that promote warping. A transversal hole through the part was included to adapt the sample to the pull-off test. The part will now be known as dolly. Two dollies were printed in each printing session and on the same PC-steel assembly (see **Figure 1f**).

2.4 Pull-off test

Immediately after the 3D printing, pull-off tests of the printed dollies were conducted. This test was based on the ISO 4624:2003 standard (see **Figure 1g** and **1h**). A TRIAX-50 (Controls) machine with a 200 N load cell was used to measure the strength required to detach the dollies from the PC base (hereafter breaking strength) (see **Figure 2c**).

Each sample (PC-steel assembly with two printed dollies) was attached to the mobile platform of the machine. Subsequently, a hook-like tool was inserted through the dolly's transversal hole. This hook was attached to the load cell. When all components were in contact with each other (PC-steel assembly, dolly, hook and load cell), the mobile platform moved downwards at 2 mm/min and the breaking strength that was recorded by the machine until the dolly separated from the PC printing base. The maximum value of the breaking strength was reached when a sudden take-off of the POM part from the PC printing base took place. This value was interpreted as the breaking strength of each sample. Then, the breaking strength force in newtons was divided by the area of the dolly (692.21 mm^2) to obtain the breaking tensile strength in kPa. The average value of eight measurements for each treatment configuration was used as the breaking strength to study the adhesion.

2.5 Chemical characterization

The chemical characterization of the coatings was determined by X-ray Photoelectron Spectroscopy (XPS) analyses. X-ray photoelectron spectra were obtained by use of a Kratos AXIS Supra spectrometer with a multi-channel hemispherical analyzer and a Monochromatic AlKα X-ray source (225 W, 15kV, 1486.69 eV). The energy scale was calibrated using Cu 2p3/2, Ag 3d5/2 and Au 4f7/2 at 932.7, 368.3 and 84.0 eV, respectively. The spectra were

acquired at a constant pass energy of 160 eV (general spectra) and 20 eV (high-resolution spectra). The base pressure of the instrument was below 1.33×10^{-7} Pa. *Kratos ESCApe* and *CasaXPS* software were used for the acquisition and analysis of the data, respectively. A 285 eV binding energy for the C1s signal of the adventitious carbon was used to reference the peaks of the samples. The C1s signal of the XPS spectra of the treated samples were deconvoluted by means of *PeakFit 4.12* (*SPSS Inc*.) software.

2.6 Wettability

In order to determine the effect of plasma treatments on the wettability of the PC surface of the studied samples, the static water contact angle (WCA) of the PC sheets of both plasma treated and non-treated samples was measured by the sessile drop method. 10 µl droplets of distilled water were dropped on the surface of each sample and the WCA was calculated by means of the OCA15 plus system (Dataphysics) and SCA200 software according to UNE EN 828:2013 standard. Each value was averaged from four measurements regarding as average WCA value of the sample.

2.7 SEM and AFM analysis

The surface of each sample was examined by a Scanning Electron Microscope (SEM) HITACHI S-2400 at an operating voltage of 18 kV. The samples that were analyzed were made conductive by gold-palladium sputtering before introduction to the SEM chamber to prevent charging, minimize radiation damage and increase electronic reflectivity during SEM analysis.

Veeco Multimode Atomic Force Microscopy (AFM) was used to explore the surface topography of the studied samples. Areas of 20 µm × 20 µm were scanned with a scanning frequency of 50 Hz. The image analysis was conducted by means of NanoScope Analysis 1.4 software.

2.8 Deformation measurement

Plasma treatment can produce undesirable side effects on the performance of the treated material.[25] In this work, the appearance of geometric deformations in treated PC sheets were observed when the PC sheet was unscrewed from the stainless steel plate.

The application of a plasma jet at temperatures that exceed ambient temperature (around 50-100ºC) on a PC substrate produces a temperature difference between the treated and the untreated surfaces that, according to Koski et al., produces a thermal stresses of a compressive nature.[23] They also observed that, as the energy was that was applied increased, so did the thermal residual stresses. Consequently, it is common to observe an increment in the sample curvature by the size of residual stresses (the greater the residual stresses, the higher the sample's curvature). We hypothesized that the residual stresses that were produced after the plasma treatment could have affected the adhesion of the POM to the PC sheet during the printing process. In this way, the residual stresses were sized. One primary method that was used to quantify residual stresses on a polymer flat sheet consists of measuring the curvature of the samples before and after applying the deformation mechanical or thermal load.[35] Once the sample is free of constraints, it restores equilibrium by warping to a shape that resembles somewhat a circular arc.[23,36]

In our particular case, the PC sheet was unscrewed from the stainless steel plate by one of its ends and, after warping. Then, the arrow was measured at the opposite end by a gauge (see **Figure 4**).

Figure 4. PC sheet deformation after constraints were released: [a] untreated PC and [b] F40.

3 Result and discussion

3.1 Analysis XPS and Wettability

An XPS analysis was conducted to determine the atomic chemical composition of the PC surface, that is, to determine the plasma treatment's influence on the degree of surface

oxidation. **Table 3** shows the functional groups and binding energies that are associated with peaks that correspond to the deconvolution of C1s high-resolution spectra (see **Figure 5**) of the untreated and plasma treated PC samples. Both, the global spectrum and the chemical components were similar to those identified by other authors.[37–39]

The plasma treatment of the PC surface resulted in the emergence of new functional groups that were based on both oxygen (C-O, C=O, O-C=O, O-C-O, COOH) and nitrogen (C=N, C-N). The higher was the power, the lower was the ionized gas flow or the greater was the exposure time (lower plasma jet speed or the greater the number of passes), the greater was the quantity of these groups. However, the original PC functional groups (C-C, C-H, C-O, CO_3 y π-π*) decreased. This chemical modification was probably due to the oxidation of the PC surface, which was caused by both plasma energy and the oxygen from the atmosphere surrounding the sample. The emergence of these new functional groups was expected to be critical to the increase of the POM adhesion.[28]

Component	Functional group	Binding energy (eV)	Reference
A	C-C C-H	~285	[37–39]
B	C=N	~285.6	[40,41]
C	C-O C-N	~286.5	[37–39]
D	C=O O-C=O	287.6 - 288.6	[28,42]
E	O-C-O COOH	289.3 - 290	[37]
F	CO_3	~291	[37–39]
G	π-π*	~291.7	[37–39]

Table 3. Functional groups and binding energies associated with peaks that corresponds to the deconvolution of C1s spectra.

Figure 5. Deconvolutions of C1s spectra of samples: [a] untreated PC, [b] S30, [c] S20, [d] S50, [e] F40, [f] F80, [g] W300 and [h] P3.

In this sense, static water contact angles (WCA) were measured to determine the wettability of the PC surface. This property is related to the increase adhesion.[28] **Figure 6** shows the WCA images of some analyzed samples. Depending on the plasma treatment applied to the PC surface, a great difference in hydrophilic character was observed. The WCA of plasma treated samples was lower than those of untreated PC. The surface of the untreated PC exhibited a WCA of 72.6º ± 2.9, whereas the WCA of the plasma treated samples ranged between 10-30º. That is, the plasma treatment of PC surfaces caused an increase in the hydrophilic character.

Figure 6. WCA of samples: [a] untreated PC, [b] S30, [c] F40, [d] W300, [e] P3 and [f] F80.

Figure 7 depicts the percentage of the oxygen-based functional groups and the WCAs for each plasma treatment configuration. The oxygen-based functional groups that appear in **Figure 7** are the sum of "D" and "E" components of **Table 3**. In general, one can identify an inverse relationship between the WCA and the degree of oxidation of the PC surface. That is, the greater the plasma exposure (lower plasma jet speed, lower gas flow, higher power and higher number of passes), the greater are the oxygen-based functional groups and the lower the WCA (greater hydrophilicity).

Figure 7. Percentage of oxygen-based functional groups and WCAs for all the plasma treatments.

3.2 Adhesion

The adhesion of the 3D printed sample to the PC sheet was determined in terms of the breaking strength of the samples in pull-off tests. This was done to establish a relationship

between the degree of surface oxidation and the adhesion of samples. **Figure 8** shows the distribution of functional groups based on oxygen (%) and the breaking strength (kPa) for the different plasma treatments that were analyzed in this work. The dashed line indicated the breaking strength of non-plasma treated sample. One can note that, with the exception of the F40 sample, all plasma treatments improved the POM first printed layer adhesion to the PC sheet in comparison to the non-plasma treated one. Sample S30 revealed an improvement in adhesion of 45% (breaking strength of S30: 161.14 kPa vs. breaking strength of non-plasma treated PC sheet: 111.43 kPa).

Considering the breaking strength distribution (adhesion) of samples in **Figure 8**, it can be seen, in general, that the higher the plasma jet speed is, the lower the breaking strength is. This trend is not true at very low speeds (20-25 mm/s). It must be noted that there is a limit at which the reduction of the plasma jet speed and the consequent increase in the exposure time to plasma does not guarantee an increase in the adhesion of POM. Similarly, when the plasma power was modified, one can see a linear tendency. In other words, the higher the plasma power is, the greater the POM adhesion is. Related to the gas flow, the adhesion was studied extensively, since different gas flows resulted in significant variations of the first printed layer adhesion of POM. When high gas flows were used (sample F80), the adhesion improved slightly as these treatments resulted in a low ionized plasma and, therefore, a low percentage of oxygen-based functional groups. Low gas flows (sample F40), which lead to a highly energetic plasma, caused wide cracks which resulted in a high breaking strenght and, in consequence, leaded to a PC surface with a non-desired adhesion (see Figure 9f and 10f). In this particular case, the adhesion was poorer than for the non-plasma treated sample. A similar situation was observed when the number of passes was varied. The highest adhesion was reached just with one plasma pass. Therefore, an increase in plasma exposure time does not guarantee greater adhesion.

Taking into account the abovementioned findings, it can be concluded that different relationships were observed after studying the degree of surface oxidation and the breaking strength of samples. In general, an increase in the degree of oxidation of the PC surface leads to an increase in the first printed layer adhesion of POM on the PC sheets with the exceptions of samples F40, P2 and P3. An explanation of these exceptions is provided below.

Figure 8. Distribution of functional groups based in oxygen (%) and the breaking strength (kPa) for all the plasma treatments.

3.3 SEM and AFM Analysis

SEM and AFM analyses were undertaken to observe the surface modifications that were caused by plasma treatments on PC sheets. This involved a study of the morphology of the treated PC sheets. **Figure 9** illustrates some representative SEM images of PC sheets. It may be note that the lowest power plasma treatment (sample W300) caused a superficial cleaning in comparison to the untreated PC sheet. This may be related to the slight adhesion improvement of this sample. However, stronger plasma treatments (lower plasma jet speed, higher number of passes and lower gas flow) caused the appearance of cracks, wider and longer with lower gas flows (sample F40) and a greater number of passes (sample P3).

Figure 9. SEM images of samples: [a] untreated PC, [b] S30, [c] S20, [d] W300, [e] P3 and [f] F40.

AFM images of the representative samples analyzed are shown in **Figure 10**. As can be seen, the SEM and AFM images of the same sample were quite similar. As mentioned above, the most powerful plasma treatments (S20, P3 and F40) caused a superficial modification with some cracks.

Figure 10. AFM images of samples: [a] untreated PC, [b] S30, [c] S20, [d] W300, [e] P3 and [f] F40.

The morphological and superficial modifications that were caused by powerful plasma treatments seemed to damage the PC surface. However, it should be noted that the lower adhesion of these samples (lower than expected, if considering their high degree of oxidation) cannot be related only to this superficial damage. The appearance of cracks on the surface of the PC sheets probably was due to the creation of residual stresses by the plasma energy that was applied. This idea is explained further in the next section.

3.4 Deformation

In **Figure 4b** and **11**, one can see the geometric deformations that were caused by thermal residual stresses on the treated PC samples. The higher curvature of the PC samples are associated with the most powerful plasma treatments. Specifically, samples P2, P3 and F40 showed the greatest deformation (P2: 4.01 ± 0.37 mm; P3: 4.48 ± 1.15 mm; and F40: 6.63 ± 2.23 mm). This result is in concordance with the work of Koski et al. who observed that, as the plasma exposure increased, the compressive thermal stresses on the substrate treated surface rose.[23]

As was stated in previous sections, theses samples (P2, P3 and F40) showed a low adhesion, despite exhibiting a large number of oxygen-based functional groups (see Figure 8). Therefore, there is a relationship between residual stresses and adhesion properties. Koski et al. also related the presence of residual stresses on a PC sheet as a cause of adhesion reduction between a coating and its PC substrate.[23] Similarly, other authors concluded that the surface residual stresses of the PC substrate could affect the adhesion properties of thin films.[25,27]

In our particular case, there also could be another deformation mechanism acting on a micro scale. Ram et al. exposed the impact of temperature on the magnitude and type (tensile or compressive) of residual stresses on PC samples.[43] They verified that changes in temperature

could reverse the types of residual stresses near the sample's surface. As was explained in the experimental section, POM material was extruded on the substrate surface as a molten filament at a temperature of about 250ºC. This temperature is fairly higher than the PC glass transition temperature (147 ºC). Thus, the deposited filament at a high temperature could cause micro modifications of the surface geometry that allow stress relaxation and residual stresses size and type alterations. The higher the residual stresses are, prior to the POM filament deposition, the greater are the alterations. These could produce a reduction in adhesion between POM and the PC substrate. However, further investigation of this aspect is necessary and will be undertaken in future research.

Figure 11. Deformation distribution of PC sheet for different plasma treatments.

In view of the results, it can be concluded that samples that were exposed to powerful plasma treatments exhibited greater deformations of the PC sheet. This effect, together with the appearance of surface cracks in samples P3 and F40 made the improvement in chemical composition of the PC sheet insufficient to improve the adhesion of the first printed layer of POM.

4 Conclusions

A deeply study had to be performed since plasma treatment that one could think to be more efficient (those that generate many adhesive chemical bonds) were no effective in this particular application, since they release surface tensions, which result in a bad adhesion. Finally, a plasma treatment has been successfully applied to PC sheets with the aim of improving the adhesion of the POM material in 3D printing. In fact, nearly all plasma configurations that were used in this work had a breaking strength that was higher than that of a non-plasma treated PC sample.

Sample S30, treated with 1 pass of plasma at 500 W of power, a plasma jet speed of 30 mm/s and an air flow of 60 slm, increased the adhesion by 45% with respect to the non-plasma treated PC sample (breaking strength of S30: 161.14 ± 33.86 kPa and untreated PC: 111.43 ± 26.93 kPa).

It is worth mentioning that, in general, the adhesive capacity improved with a decrease in plasma jet speed and the increase of plasma power. In contrast, the higher the number of passes or the lower the gas flow, the worse the adhesion was. With regard to the XPS analyses, it was observed that the greater the energy of the plasma treatment, the greater was the chemical modifications on the PC surface and a consequent increase of the oxygen-based functional groups. Overall, an increase in the oxidation degree of the PC surface led to an increase in adhesion. However, samples P2, P3 and F40, which showed the highest oxygen percentage in their atomic chemical composition, suffered morphological damage. This was evidenced by the SEM and AFM images of these samples, in which surface cracks were observed. However, these cracks were not considered as a sole cause for the adhesion loss, but as possible evidence of the appearance of thermal residual stresses. A relationship between the plasma exposure and the PC substrate residual stresses was found in terms of decrease of adhesion.

Finally, in regards to the WCA tests, a direct relationship between the plasma exposure and the wettability was found. That is, the greater the degree of plasma exposure, the more hydrophilic was the PC surface. This relationship resulted, in general, in a higher adhesion.

In future research, substrates that differ from PC and plasma gases that differ from compressed air will be tested. In addition to this, the influence on the POM adhesion of different printing parameters like the extruder temperature and the printing base temperature will be deeply study.

Acknowledgements: This work was funded by the *Programa Estatal de Investigación, Desarrollo e Innovación Orientada a los Retos de la Sociedad* through the project AGL2017-

82779-C2-1-R. XPS tests were conducted by the "Advanced Microscopy Laboratory (LMA)" of "The Institute of Nanocience of Aragon (INA) - University of Zaragoza". The authors would like to thanks LMA-INA for access to their equipment and their expertise. The authors also wish to thanks the *Área UR-Maker* of the University of La Rioja for the access to the 3D printer that was used in this research. The author, E. Sainz-García, as postdoctoral researcher of the University of La Rioja, thanks the postdoctoral training program that is funded by the *Plan Propio* of the University of La Rioja and the *V Plan Riojano de I+D+i* of the Autonomous Community of La Rioja.

Received: ((will be filled in by the editorial staff)); Revised: ((will be filled in by the editorial staff)); Published online: ((please add journal code and manuscript number, e.g., DOI: 10.1002/ppap.201100001))

Keywords: 3D printing; Adhesion improvement; Atmospheric pressure air plasma; Polycarbonate; Polyoxymethylene

[1] I. Gibson, D. Rosen, B. Stucker, Additive Manufacturing Technologies, Second, Springer New York, New York, NY, 2015. doi:10.1007/978-1-4939-2113-3.

[2] D.I. Wimpenny, P.M. Pandey, L.J. Kumar, Advances in 3D printing & additive manufacturing technologies, Springer Singapore, Singapore, 2017. https://www.springer.com/gp/book/9789811008115 (accessed January 19, 2018).

[3] J. Yoders, What Materials Are Used in 3D Printing? Not Just Plastic [Updated], Redshift by Autodesk. (2018). https://www.autodesk.com/redshift/what-materials-are-used-in-3d-printing/ (accessed November 21, 2018).

[4] D.L. Jarvis, Polyacetals, Elsevier Ltd, 2017. doi:10.1016/B978-0-323-35824-8.00019-0.

[5] S. Lüftl, P.M. Visakh, Polyoxymethylene: State of Art, New Challenges and OpportunitiesLüftl, S., & Visakh, P. M. (2014). Polyoxymethylene: State of Art, New Challenges and Opportunities. In Polyoxymethylene Handbook: Structure, Properties, Applications and their Nanocomposites, in: Polyoxymethylene Handb. Struct. Prop. Appl. Their Nanocomposites, 2014: pp. 1–19. doi:10.1002/9781118914458.ch1.

[6] DuPont, DuPont ™ Delrin ® acetal resin Molding Guide, 2018.

[7] MatWeb, POM shrinkage ratio, (2018).

[8] Misumi, Molding Shrinkage Ratios of Major Plastic Materials | Technical Tutorial - MISUMI, (2018).

[9] Stratasys, 3D Printing Materials & Supplies | Stratasys, (2018). www.stratasys.com/materials (accessed January 18, 2018).

[10] L. Tokarz, S. Pawlowski, M. Kedzierski, Polyoxymethylene Applications, in: Polyoxymethylene Handb. Struct. Prop. Appl. Their Nanocomposites, 2014. doi:10.1002/9781118914458.ch5.

[11] 3D Systems, Materials | 3D Systems, (2018). https://www.3dsystems.com/materials (accessed January 18, 2018).

[12] 3DFilaPrint, Filaments, (2018).

[13] ColorFabb, ColorFabb - MATERIALS, (2018).

[14] Fillamentum, Collections – Fillamentum.com, (2018).

[15] Formfutura, Products | Formfutura, (2018).

[16] Hatchbox, Hatchbox Products, (2018).

[17] Taulman3D, A General Overview of taulman3D Materials, (2018).

[18] actifil3D, POM filament for 3D printer - Filaments imprimante 3D - ACTIFIL 3D, (2018).

[19] Apium, Advanced materiasl-POM | Apium Additive Technologies GmbH, (2018). https://apiumtec.com/en/download (accessed January 24, 2018).

[20] FFF-World, Technical documentation, (2018).

[21] Gizmo Dorks, Acetal 3D Printer Filament | Gizmo Dorks, (2018).

[22] Filaments-directory, POM filament for your 3D printer, (2018). https://www.filaments.directory/en/plastics/pom (accessed November 22, 2018).

[23] K. Koski, J. Hö Lsä, P. Juliet, Z.H. Wang, R. Aimo, K. Pischow, Characterisation of aluminium oxide thin films deposited on polycarbonate substrates by reactive magnetron sputtering, Mater. Sci. Eng. B. (1999) 94–105. www.elsevier.com/locate/mseb (accessed June 8, 2018).

[24] B.D. Tompkins, J.M. Dennison, E.R. Fisher, Etching and post-treatment surface stability of track-etched polycarbonate membranes by plasma processing using various related oxidizing plasma systems, Plasma Proces. 11 (2014) 850–863. doi:10.1002/ppap.201400044.

[25] X. Zhang, J. Lang, Y. Yan, X. Zhang, Y. Zhong, L. Li, Plasma pretreatment of polycarbonate substrates for indium zinc oxide film deposition, Surf. Interface Anal. 49 (2017) 376–383. doi:10.1002/sia.6142.

[26] J. Kelar, M. Shekargoftar, R. Krumpolec, T. Homola, Activation of polycarbonate (PC)

surfaces by atmospheric pressure plasma in ambient air, Polym. Test. 67 (2018) 428–434. doi:10.1016/j.polymertesting.2018.03.027.

[27] X. Zhang, Y. Zhong, X. Zhang, L. Li, Y. Yan, Plasma and chromic acid treatments of polycarbonate surface to improve coating-substrate adhesion, Surf. Interface Anal. 45 (2013) 1893–1898. doi:10.1002/sia.5338.

[28] R. Múgica-Vidal, F. Alba-Elías, E. Sainz-García, M. Pantoja-Ruiz, Atmospheric pressure air plasma treatment of glass substrates for improved silver/glass adhesion in solar mirrors, Sol. Energy Mater. Sol. Cells. 169 (2017) 287–296. doi:10.1016/j.solmat.2017.05.034.

[29] L.M. Leidens, Â.E. Crespi, C.D. Boeira, F.G. Echeverrigaray, C.A. Figueroa, Hydrogen plasma etching mechanism at the a-C:H/a-SiCx:H interface: A key factor for a-C:H adhesion, Appl. Surf. Sci. 455 (2018) 1179–1184. doi:10.1016/j.apsusc.2018.05.203.

[30] C. Zhang, M. Zhao, L. Wang, L. Qu, Y. Men, Surface modification of polyester fabrics by atmospheric-pressure air/He plasma for color strength and adhesion enhancement, Appl. Surf. Sci. 400 (2017) 304–311. doi:10.1016/J.APSUSC.2016.12.096.

[31] J. Zhu, H. Deng, W. Xue, Q. Wang, Effect of low temperature oxygen plasma treatment on microstructure and adhesion force of graphene, Appl. Surf. Sci. 428 (2018) 941–947. doi:10.1016/j.apsusc.2017.10.003.

[32] D. Zeniieh, A. Bajwa, L. Ledernez, G. Urban, Effect of plasma treatments and plasma-polymerized films on the adhesion of parylene-C to substrates, Plasma Process. Polym. 10 (2013) 1081–1089. doi:10.1002/ppap.201300045.

[33] Dimafix, Dimafix, (n.d.). http://dimafix.com/ (accessed December 16, 2018).

[34] Ultimaker, Ultimaker 2+ Specifications, (2018).

[35] A. Turnbull, A.S. Maxwell, S. Pillai, Residual stress in polymers - evaluation of measurement techniques, J. Mater. Sci. 34 (1999) 451–459.

doi:10.1023/A:1004574024319.

[36] M. Jaritz, C. Hopmann, H. Behm, D. Kirchheim, S. Wilski, D. Grochla, L. Banko, A. Ludwig, M. Böke, J. Winter, H. Bahre, R. Dahlmann, Influence of residual stress on the adhesion and surface morphology of PECVD-coated polypropylene, J. Phys. D. Appl. Phys. 50 (2017) 445301. doi:10.1088/1361-6463/aa8798.

[37] M.N. Kavalenka, F. Vüllers, J. Kumberg, C. Zeiger, V. Trouillet, S. Stein, T.T. Ava, C. Li, M. Worgull, H. Hölscher, Adaptable bioinspired special wetting surface for multifunctional oil/water separation, Sci. Rep. 7 (2017) 1–10. doi:10.1038/srep39970.

[38] K. Terpilowski, D. Rymuszka, L. Holysz, E. Chibowski, Changes in Wettability of Polycarbonate and Polypropylene Pretreated With Oxygen and Argon Plasma, Proc. 8th Int. Conf. MMT. (2014) 155–165. file:///F:/Mendeley Desktop/4-155-165.pdf.

[39] V. VanDelinder, D.R. Wheeler, L.J. Small, M.T. Brumbach, E.D. Spoerke, I. Henderson, G.D. Bachand, Simple, Benign, Aqueous-Based Amination of Polycarbonate Surfaces, ACS Appl. Mater. Interfaces. 7 (2015) 5643–5649. doi:10.1021/am508797h.

[40] N.K. Cuong, M. Tahara, N. Yamauchi, T. Sone, Effects of nitrogen incorporation on structure of a-C:H films deposited on polycarbonate by plasma CVD, Surf. Coatings Technol. 193 (2005) 283–287. doi:10.1016/j.surfcoat.2004.08.126.

[41] F. Zhou, B. Yue, X. Wang, X. Wu, L. Zhuge, Surface roughness, mechanical properties and bonding structure of silicon carbon nitride films grown by dual ion beam sputtering, J. Alloys Compd. 492 (2010) 269–276. doi:10.1016/j.jallcom.2009.11.063.

[42] K.G. Kostov, Y.A.A. Hamia, R.P. Mota, A.L.R. Dos Santos, P.A.P. Nascente, Treatment of polycarbonate by dielectric barrier discharge (DBD) at atmospheric pressure, J. Phys. Conf. Ser. 511 (2014). doi:10.1088/1742-6596/511/1/012075.

[43] A. Ram, O. Zilber, S. Kenig, Residual stresses and toughness of polycarbonate exposed to environmental conditions, Polym. Eng. Sci. 25 (1985) 577–581.

doi:10.1002/pen.760250911.

LIST OF FIGURES

Graphical Abstract

The use of polyoxymethylene as 3D printing material opens a completely new path for material processing due to its excellent properties. However, the adhesion of the first printed layer is a problem. In this way, an atmospheric pressure air plasma treatment applied over a polycarbonate (PC) printing base increases the adhesion of up to 45 % with respect to the untreated PC.

Ignacio Muro-Fraguas, Elisa Sainz-García, Alpha Pernía-Espinoza, Fernando Alba-Elías*

Atmospheric pressure air plasma treatment to improve the 3D printing of polyoxymethylene

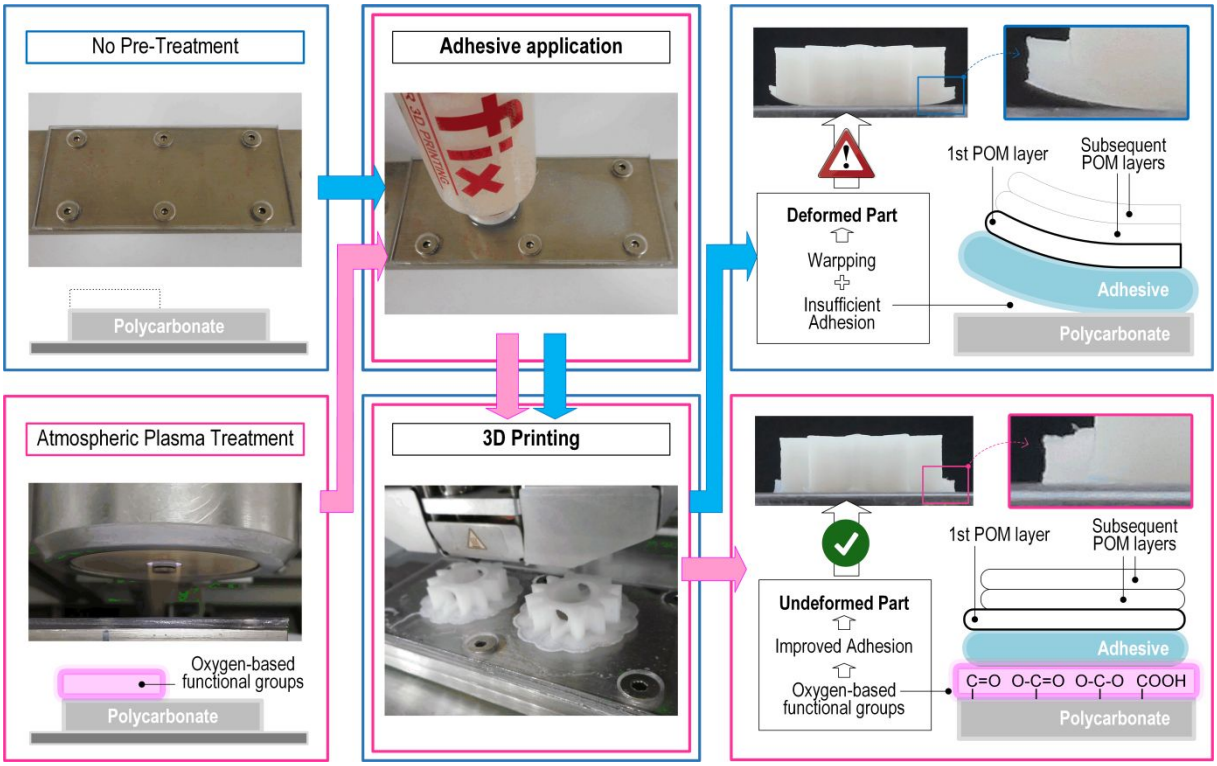

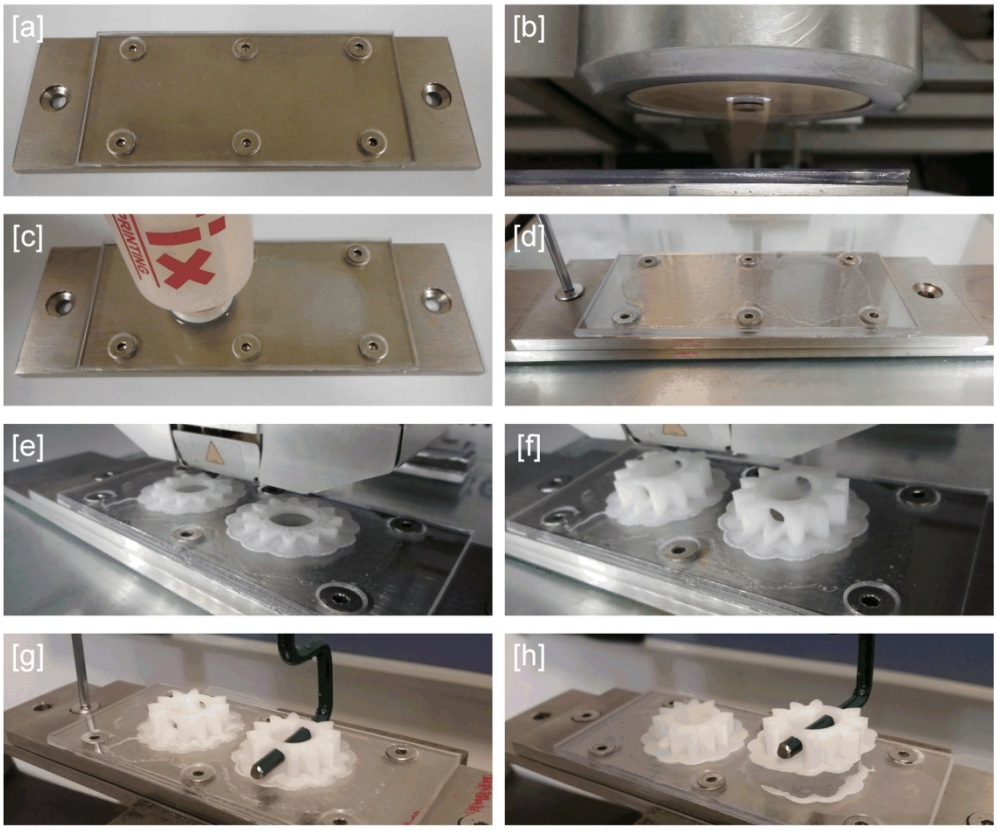

Figure 1

139x115mm (300 x 300 DPI)

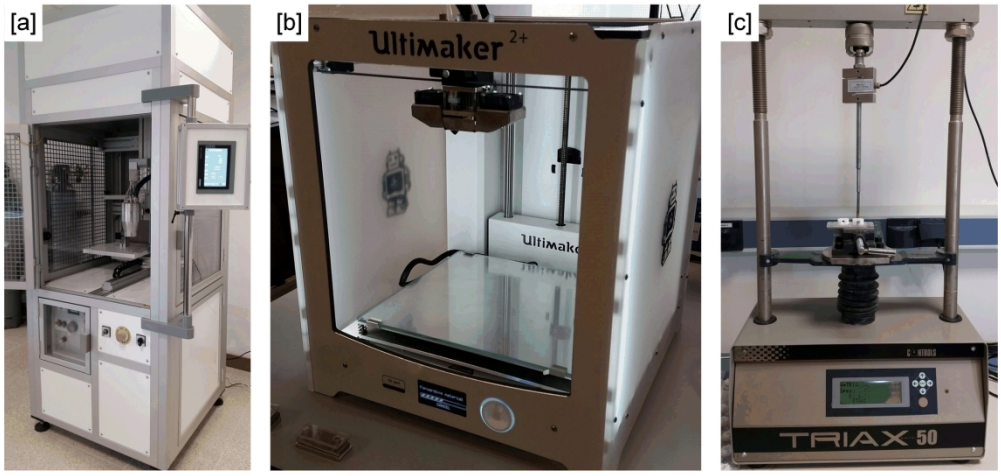

Figure 2

189x88mm (300 x 300 DPI)

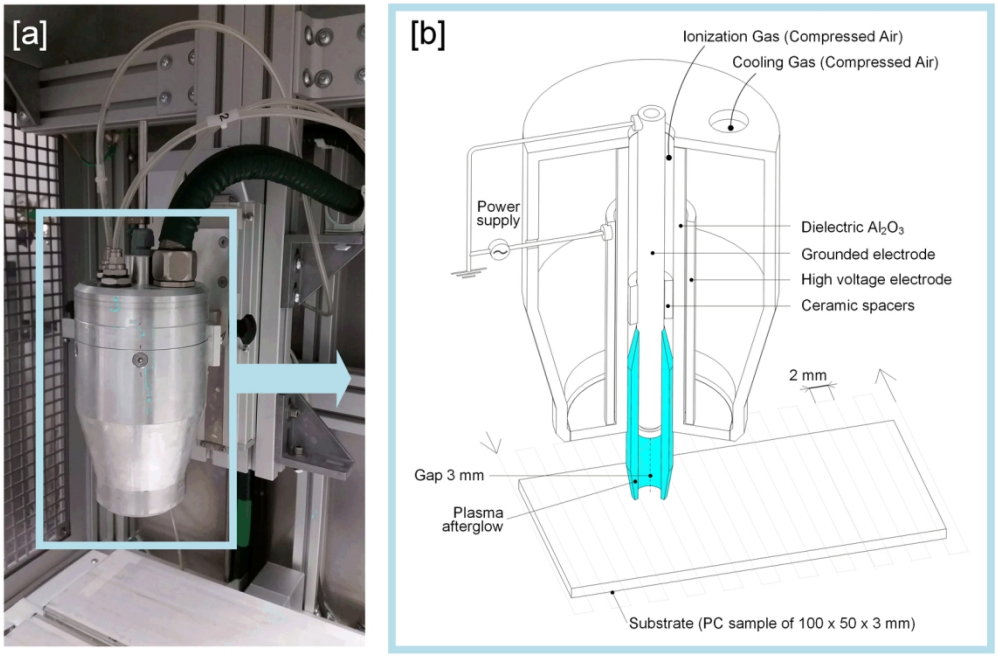

Figure 3

139x91mm (300 x 300 DPI)

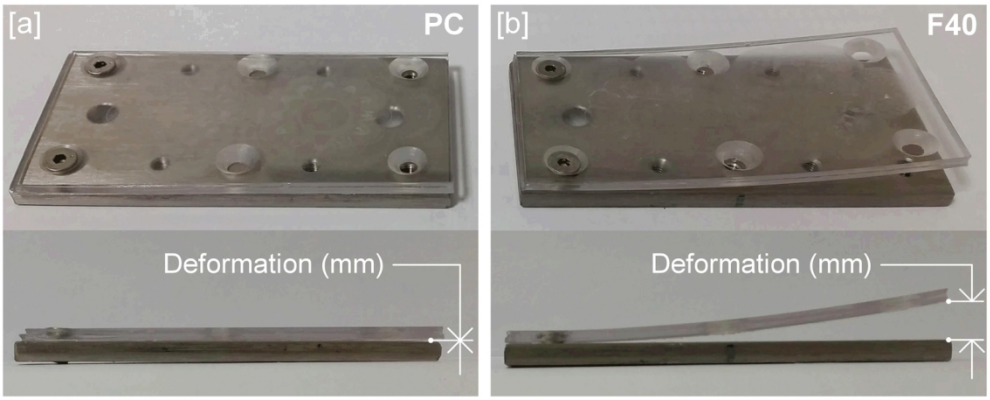

Figure 4

139x66mm (300 x 300 DPI)

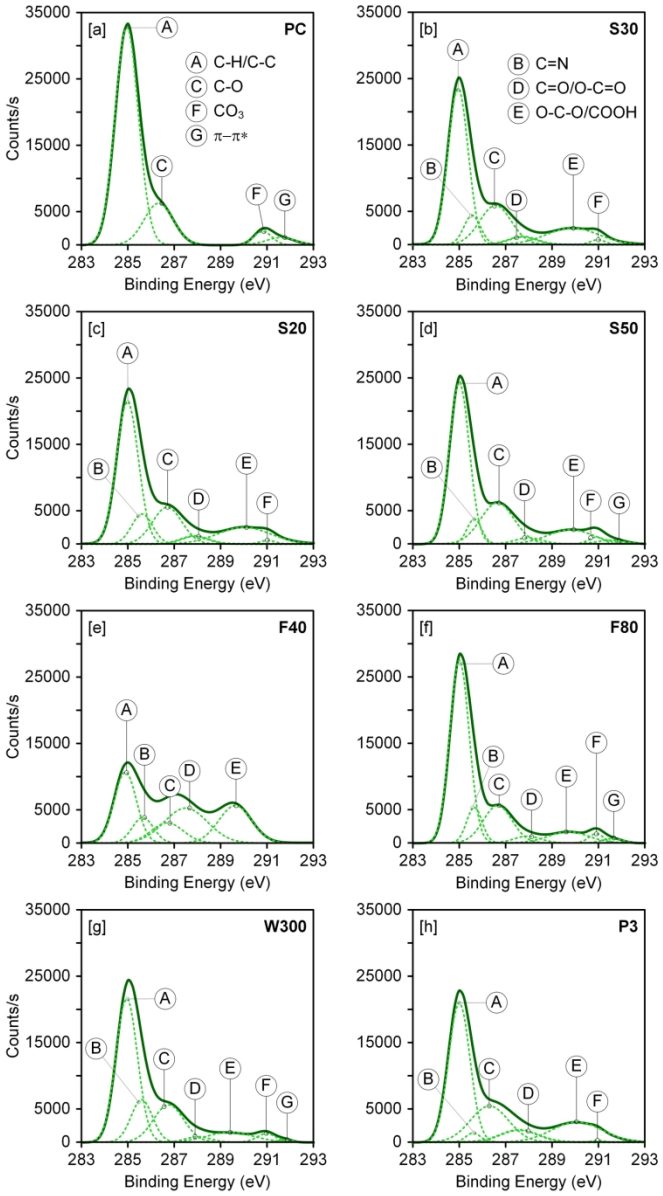

Figure 5

139x248mm (300 x 300 DPI)

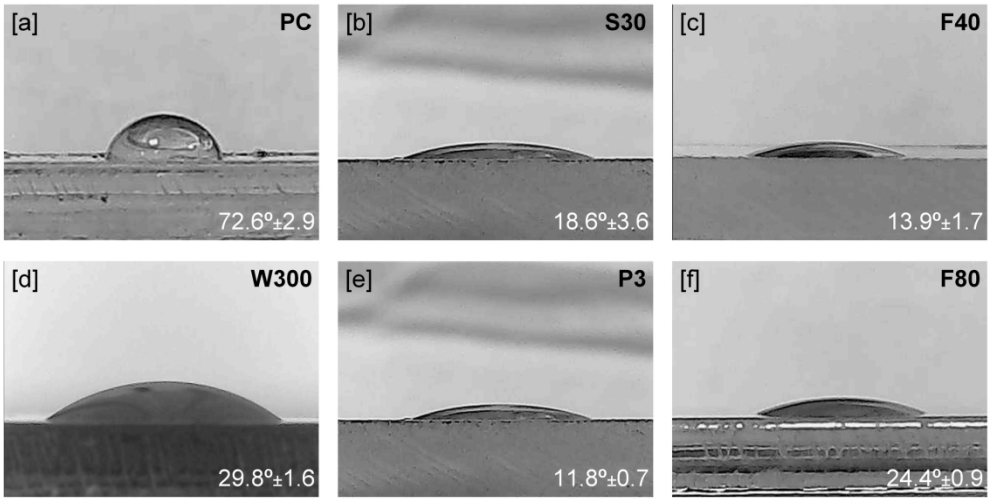

Figure 6

189x95mm (300 x 300 DPI)

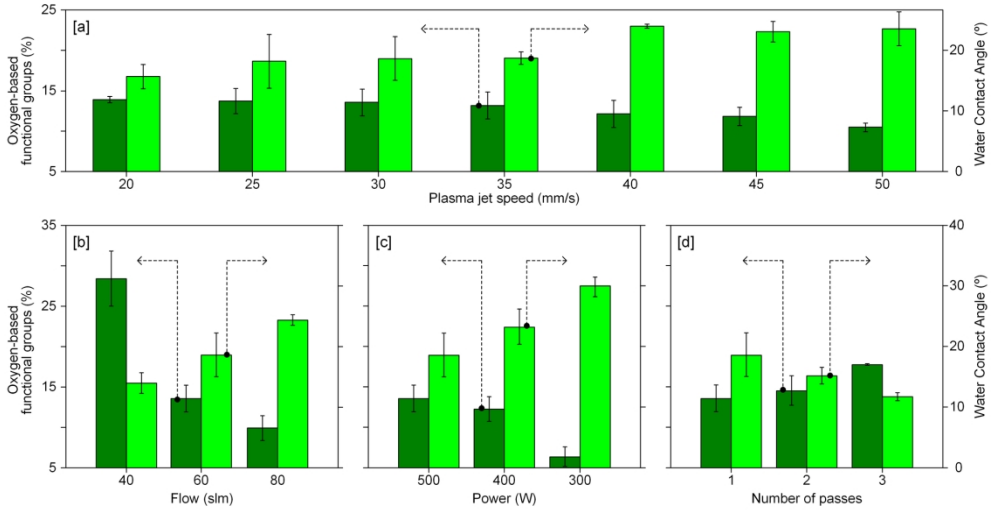

Figure 7

189x97mm (300 x 300 DPI)

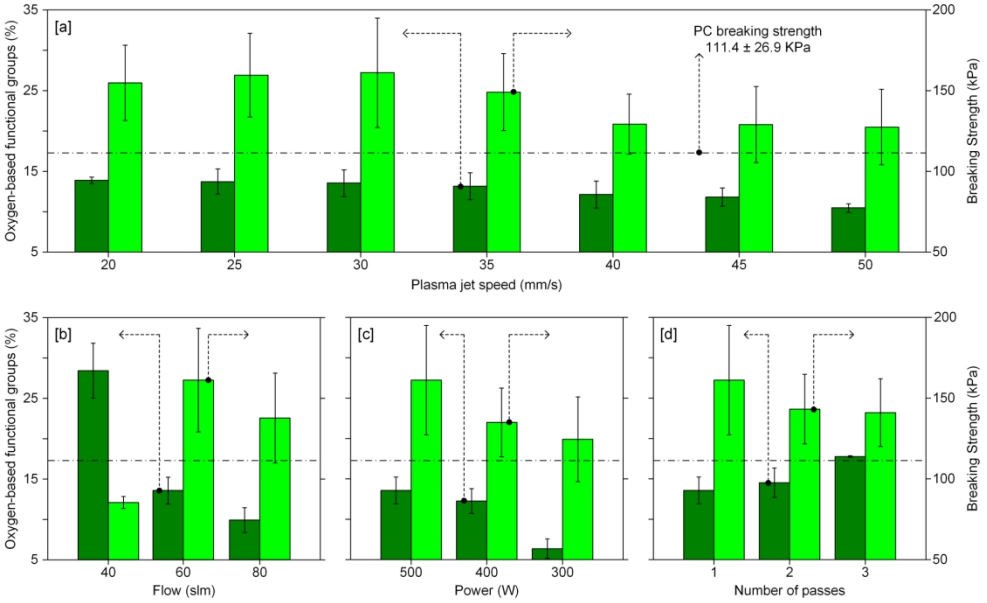

Figure 8

189x115mm (300 x 300 DPI)

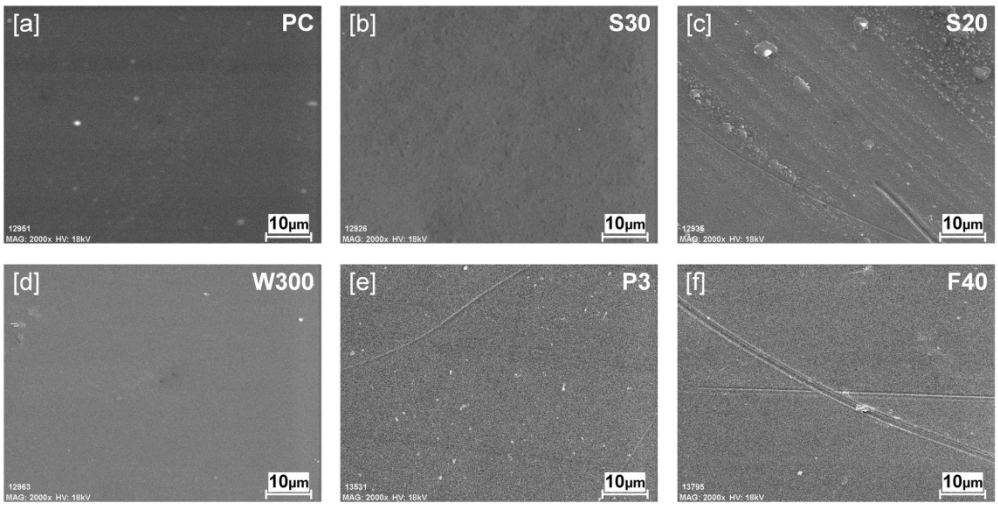

Figure 9

189x95mm (300 x 300 DPI)

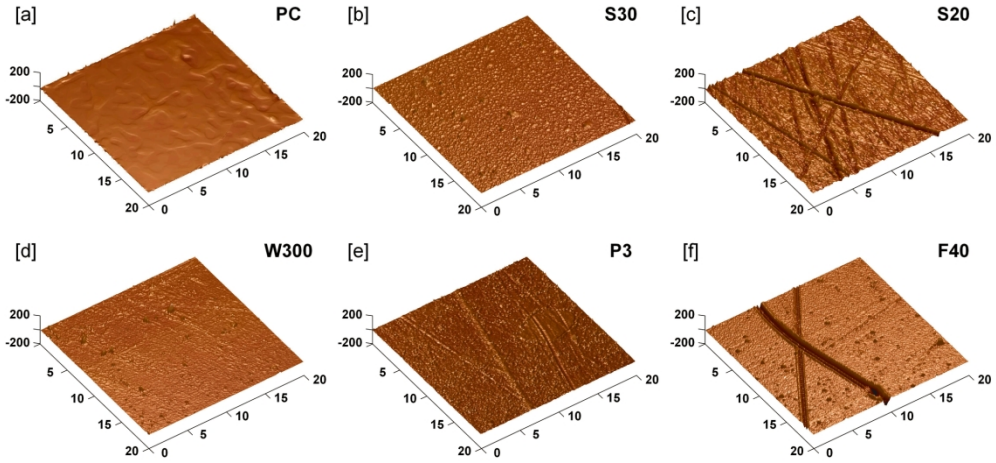

Figure 10

189x91mm (300 x 300 DPI)

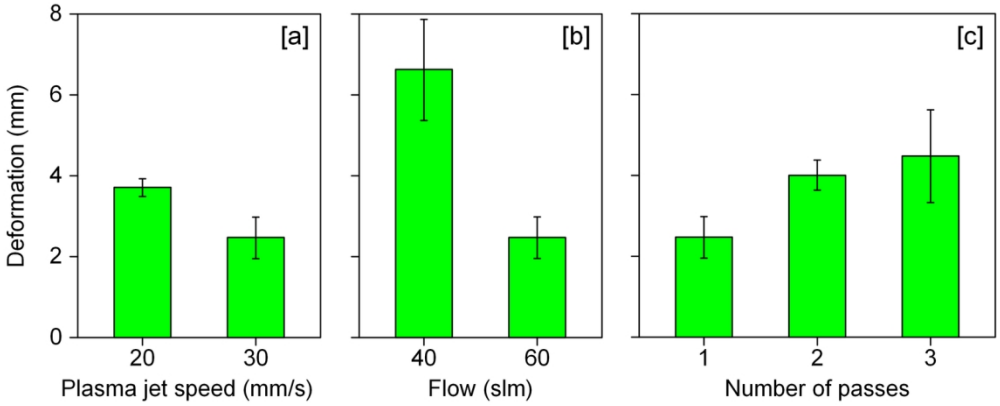

Figure 11

139x64mm (300 x 300 DPI)

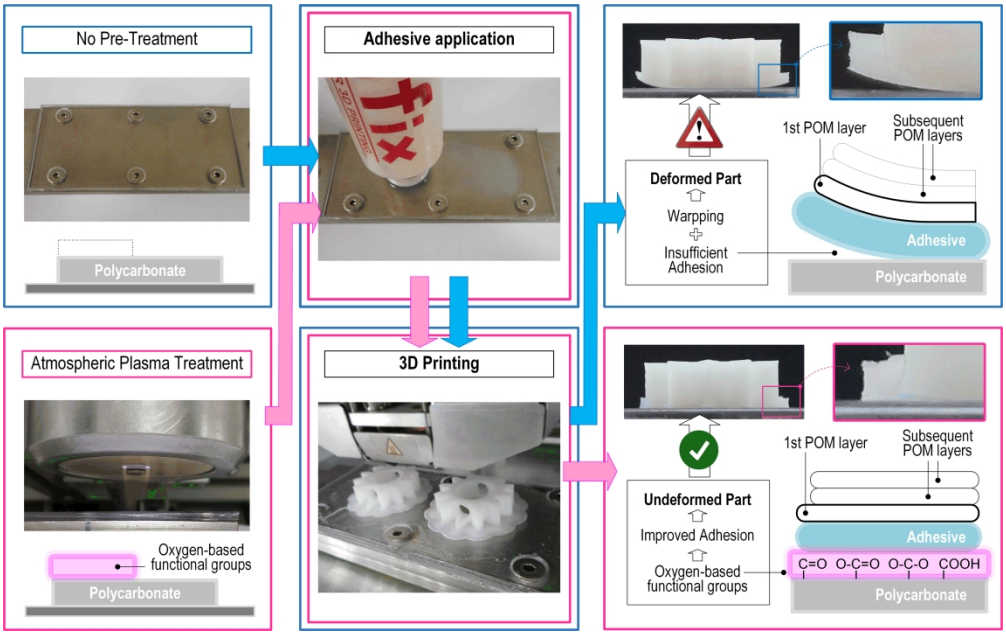

Graphical Abstract

305x191mm (300 x 300 DPI)